Do **3D Dynamic Rupture Models Capture Ground-Motion Variability** in **Long-Period Velocity Pulses**?

Insights from the 2023 Kahramanmaraş Earthquake

Rachel Preca Trapani, Mathilde Marchandon, Kadek Hendrawan Palgunadi, Baoning Wu, Ming-Hsuan Yen, Fabrice Cotton & Alice-Agnes Gabriel

Funded by the European Union

Motivation

Ground-motion (GM) variability: **combination** of different **source**, **site** and **path** effects

These are **difficult to capture** in the **near-fault** region through empirical GM models

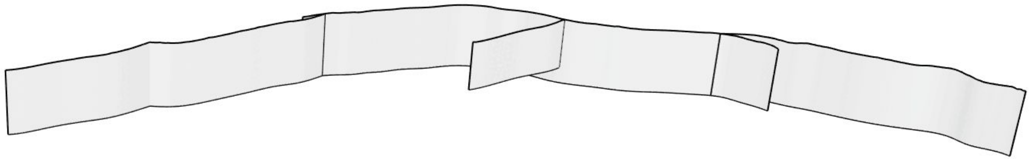

Data-constrained, **physics-based 3D dynamic rupture simulations** can help in simulating realistic GM

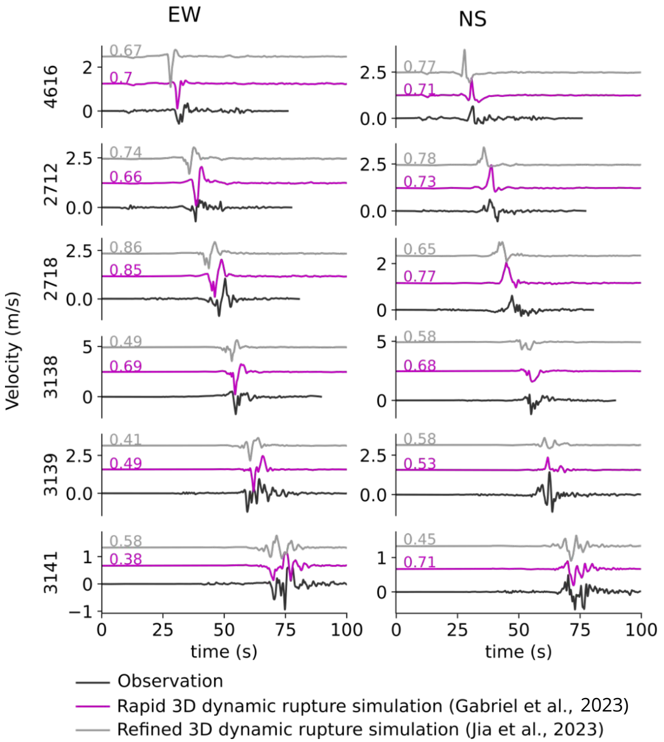

Timing & **amplitude** of ground motions are **well reproduced** to **first order**

Motivation

Pulses properties using Shahi & Baker (2014) method

(Yen et al., 2024)

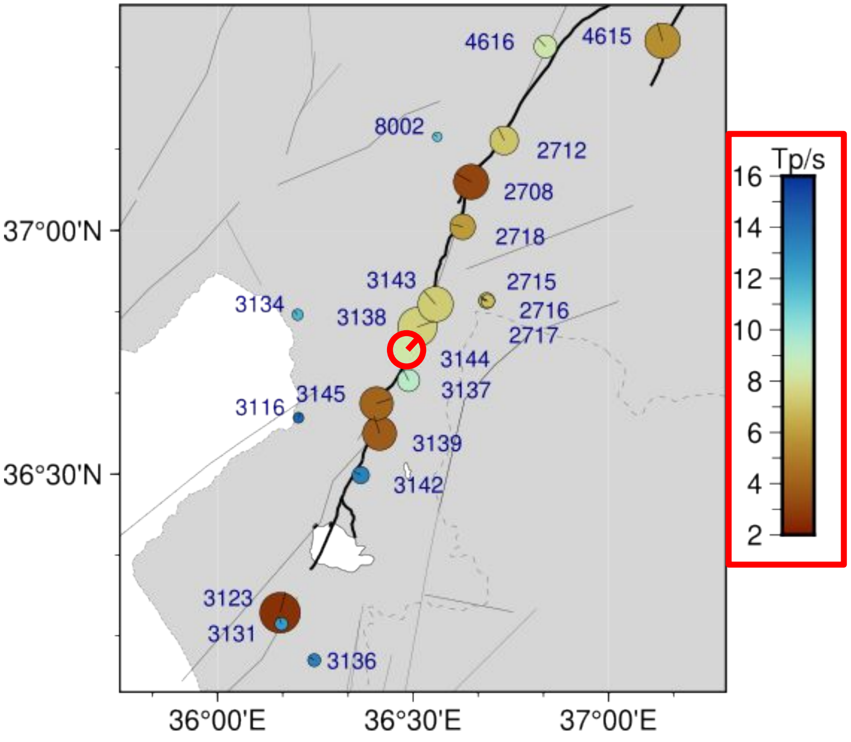

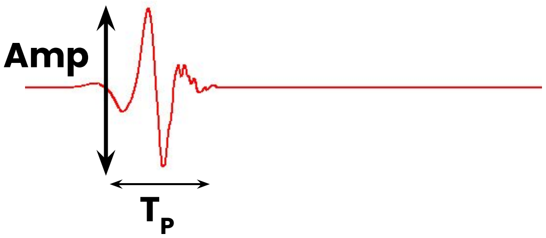

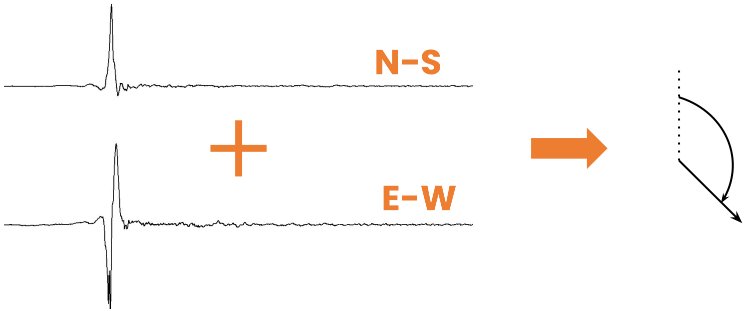

Long-period velocity pulses

- known as "**killer pulses**"-

very **hazardeous** for **near-fault structures**

Motivation

Pulses properties using Shahi & Baker (2014) method
(Yen et al., 2024)

Observation **Synthetics** (from Jia et al. 2023)

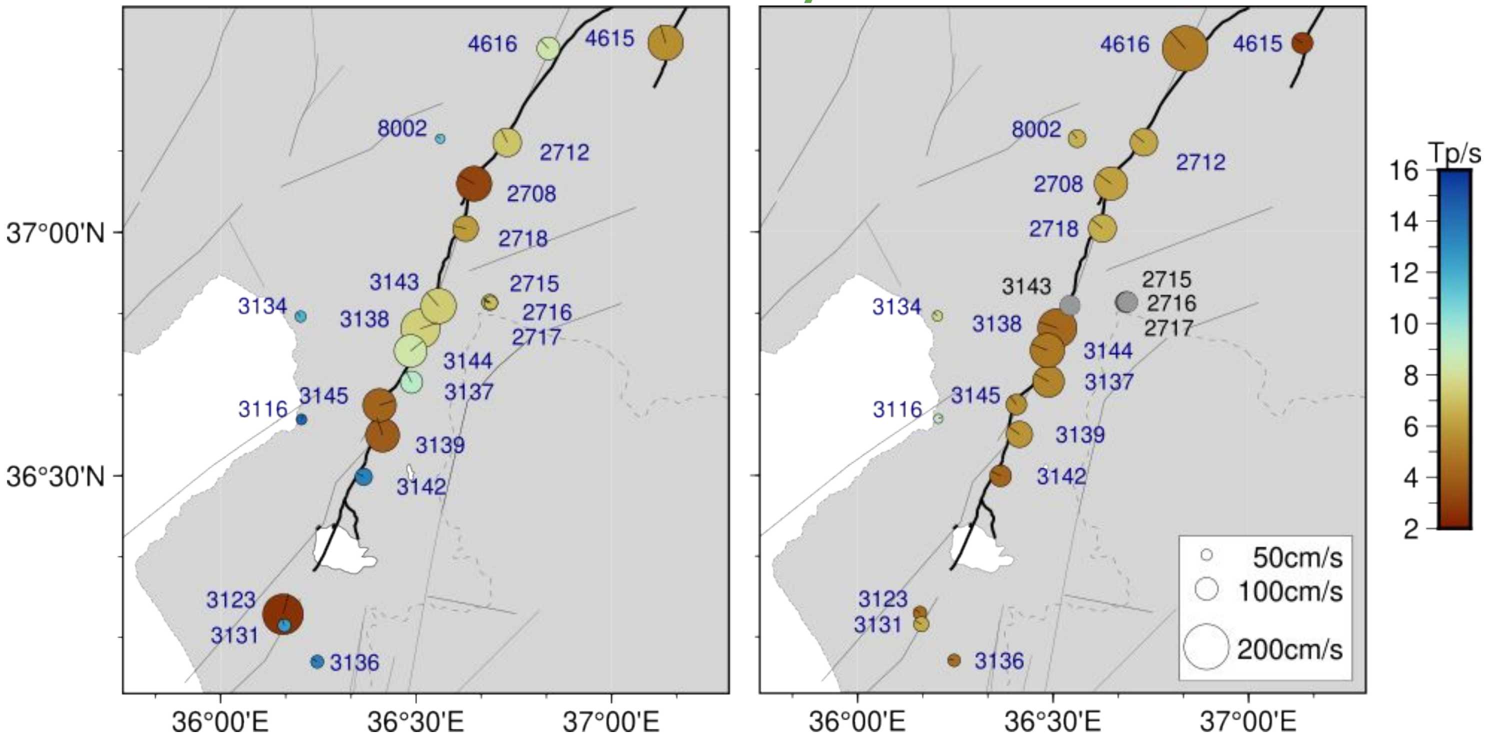

Long-period velocity pulses

- known as "**killer pulses**"-

very **hazardeous** for **near-fault structures**

Variability observed in the data is **not fully reproduced** by the **model**

What can we **add** to these models to **capture** the **ground-motion variability**?

Model Setup

3D dynamic rupture model setup follows Gabriel et al. (2023) using **SeisSol** with a focus on the **1st earthquake**

(1. Reference model)

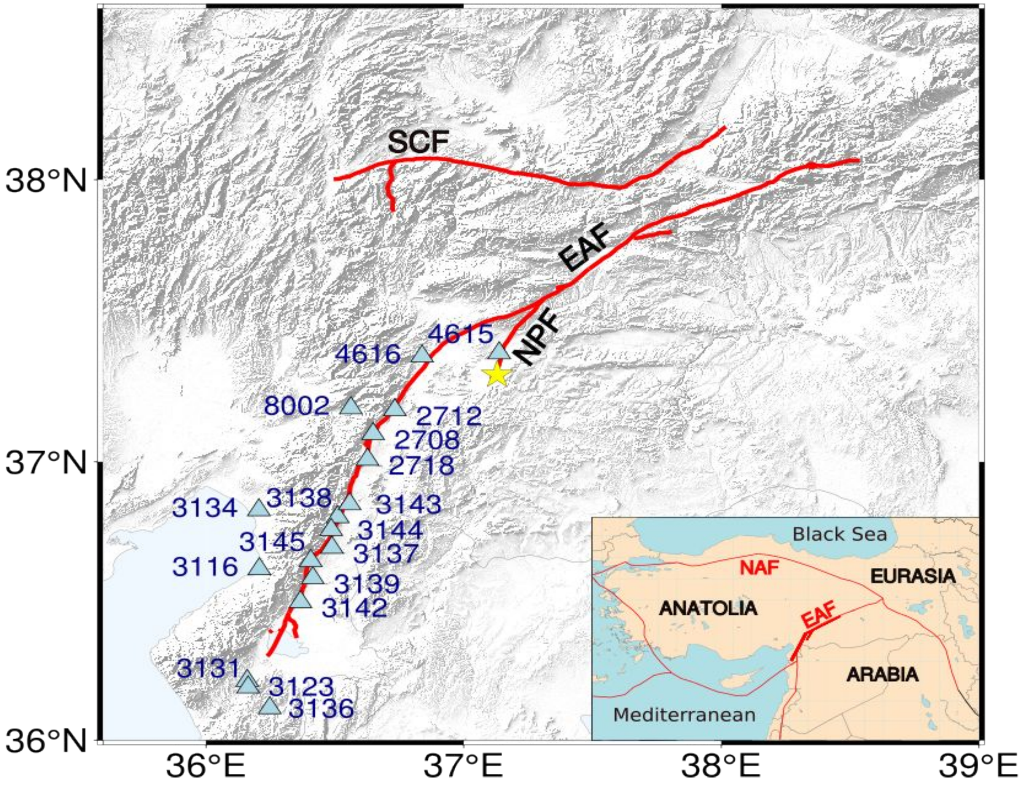

Gabriel, A., Ulrich, T., Marchandon, M., Biemiller, J., & Rekoske, J. (2023). 3D Dynamic Rupture Modeling of the 6 February 2023, Kahramanmara¸s, Turkey Mw 7.8 and 7.7 Earthquake Doublet Using Early Observations. The Seismic Record , 3 (4), 342-356.

Model Setup

3D dynamic rupture model setup follows Gabriel et al. (2023) using **SeisSol** with a focus on the **1st earthquake**

(1. Reference model)

- **Andersonian stress** with varying **SH_{max} orientations** and **pre-stress levels (R)** constrained by seismotectonics (Güvercin et al. 2022).

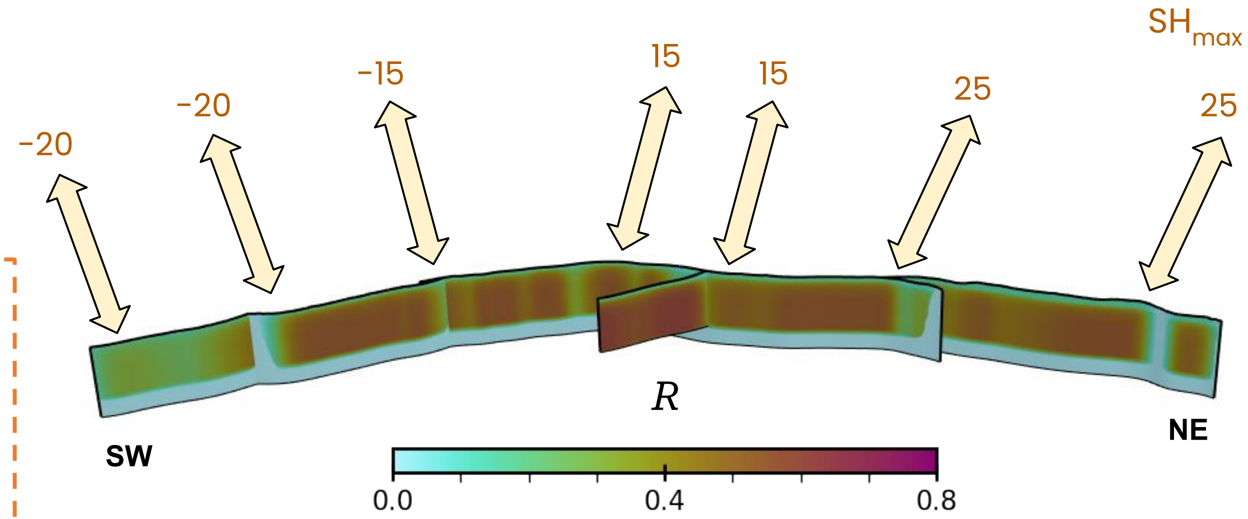

$$R = \frac{\tau - \mu_d \sigma_n}{(\mu_s - \mu_d)\sigma_n}$$

(Das & Aki, 1977)
(Aochi & Madariaga, 2003)

Gabriel, A., Ulrich, T., Marchandon, M., Biemiller, J., & Rekoske, J. (2023). 3D Dynamic Rupture Modeling of the 6 February 2023, Kahramanmaraş, Turkey Mw 7.8 and 7.7 Earthquake Doublet Using Early Observations. The Seismic Record , 3 (4), 342-356.

Model Setup

3D dynamic rupture model setup follows Gabriel et al. (2023) using **SeisSol** with a focus on the **1st earthquake**

(1. Reference model)

- **Andersonian stress** with varying **SH_{max} orientations** and **pre-stress levels (R)** constrained by seismotectonics (Güvercin et al. 2022).
- **Linear Slip-Weakening friction law with** μ_s = 0.6, μ_d = 0.2 & Dc = 0.5 m.

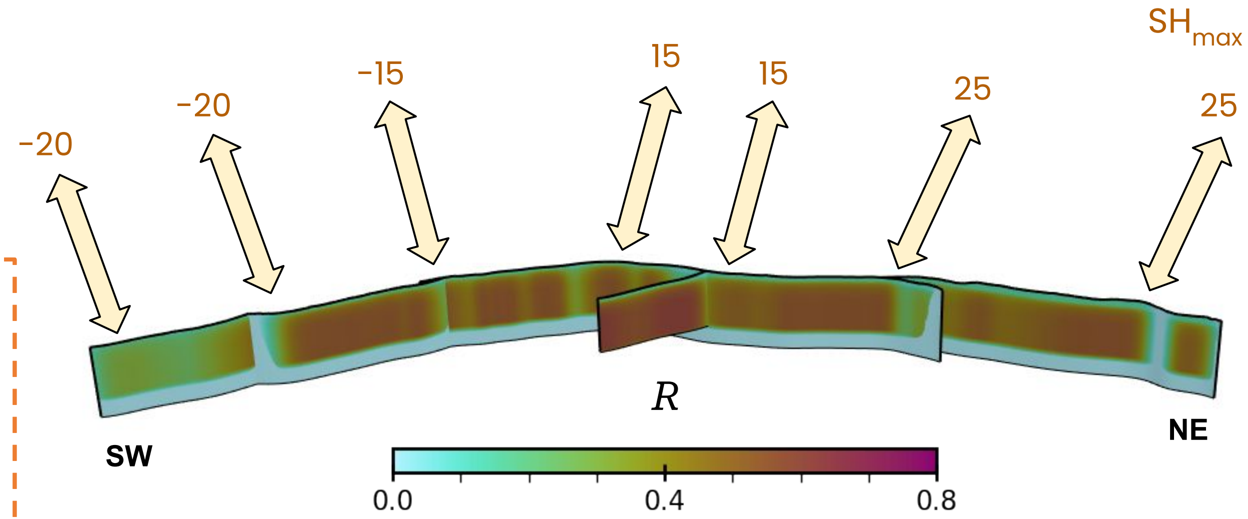

$$R = \frac{\tau - \mu_d \sigma_n}{(\mu_s - \mu_d)\sigma_n}$$

(Das & Aki, 1977)
(Aochi & Madariaga, 2003)

Gabriel, A., Ulrich, T., Marchandon, M., Biemiller, J., & Rekoske, J. (2023). 3D Dynamic Rupture Modeling of the 6 February 2023, Kahramanmaraş, Turkey Mw 7.8 and 7.7 Earthquake Doublet Using Early Observations. The Seismic Record , 3 (4), 342-356.

Model Setup

3D dynamic rupture model setup follows Gabriel et al. (2023) using **SeisSol** with a focus on the **1st earthquake**

(1. Reference model)

- **Andersonian stress** with varying **SH_{max} orientations** and **pre-stress levels (R)** constrained by seismotectonics (Güvercin et al. 2022).
- **Linear Slip-Weakening friction law with** μ_s = 0.6, μ_d = 0.2 & Dc = 0.5 m.
- The **elastic and plastic properties** of the medium are constrained by the **1D velocity model** of Güvercin et al. (2022).

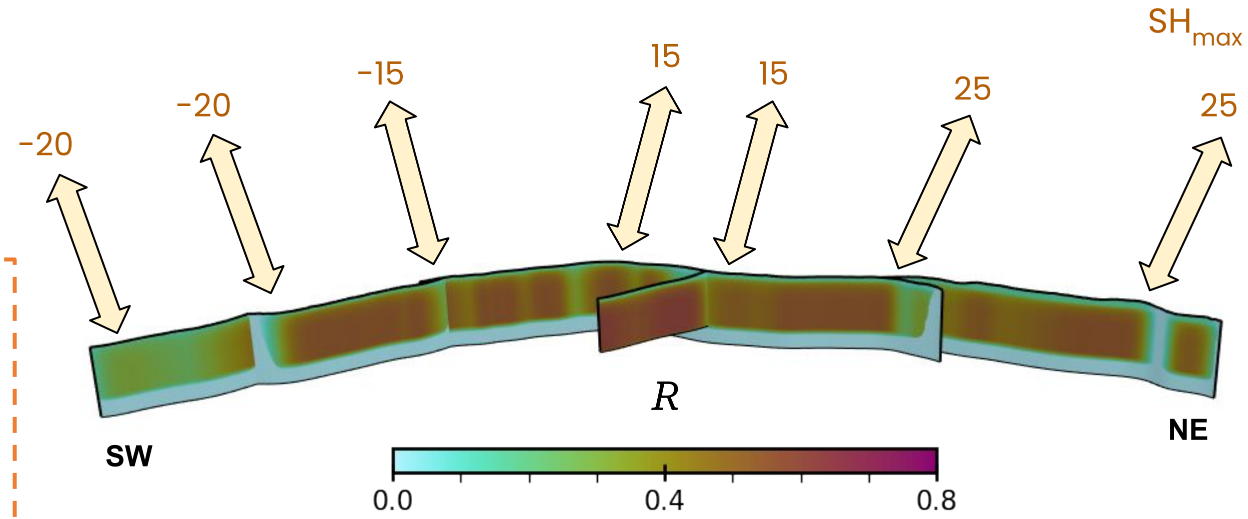

$$R = \frac{\tau - \mu_d \sigma_n}{(\mu_s - \mu_d)\sigma_n}$$

(Das & Aki, 1977)
(Aochi & Madariaga, 2003)

Gabriel, A., Ulrich, T., Marchandon, M., Biemiller, J., & Rekoske, J. (2023). 3D Dynamic Rupture Modeling of the 6 February 2023, Kahramanmaraş, Turkey Mw 7.8 and 7.7 Earthquake Doublet Using Early Observations. The Seismic Record , 3 (4), 342-356.

Added Ingredients

Reference Model

2 **Supershear initiation** model:
increased relative pre-stress ratio **(R)** on the **splay Nurdaği-Pazarcik Fault**

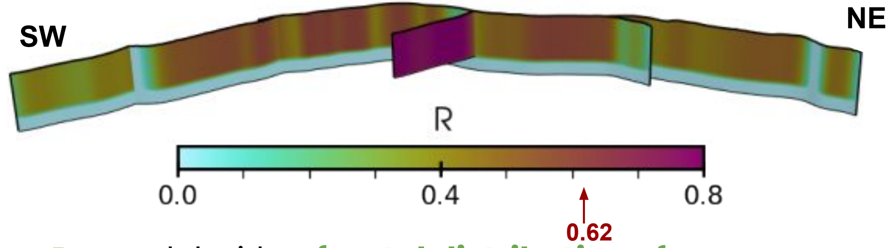

4 **D_c** model with a **fractal distribution of heterogeneous D_c** following Ide & Aochi (2005)

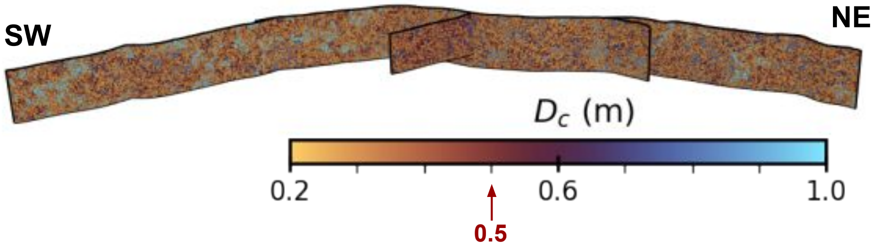

6 **Waviness** model with defined **large-scale on-fault roughness**

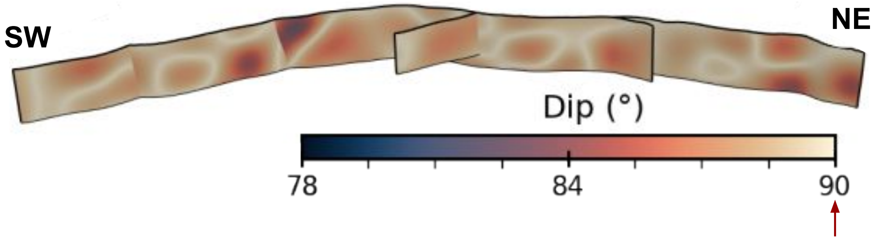

3

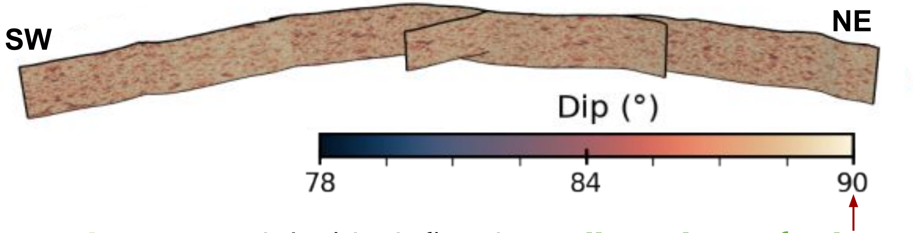

Roughness model with defined **small-scale on-fault roughness**

5 **μ_d** model with a **distribution of heterogeneous μ_d** following Ide & Aochi (2005)

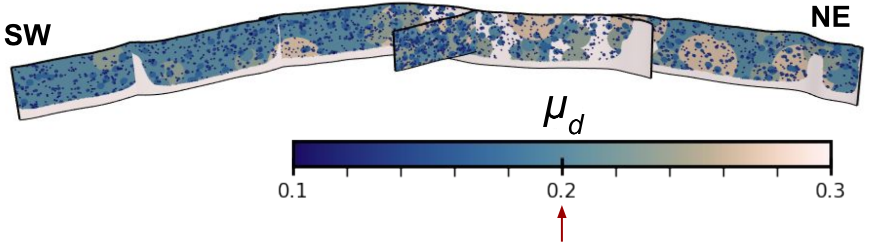

Pulse **amplitude variability** is **captured** well

Pulse Property Analysis Maps

Some pulse **period** and **orientation variability** is **captured**

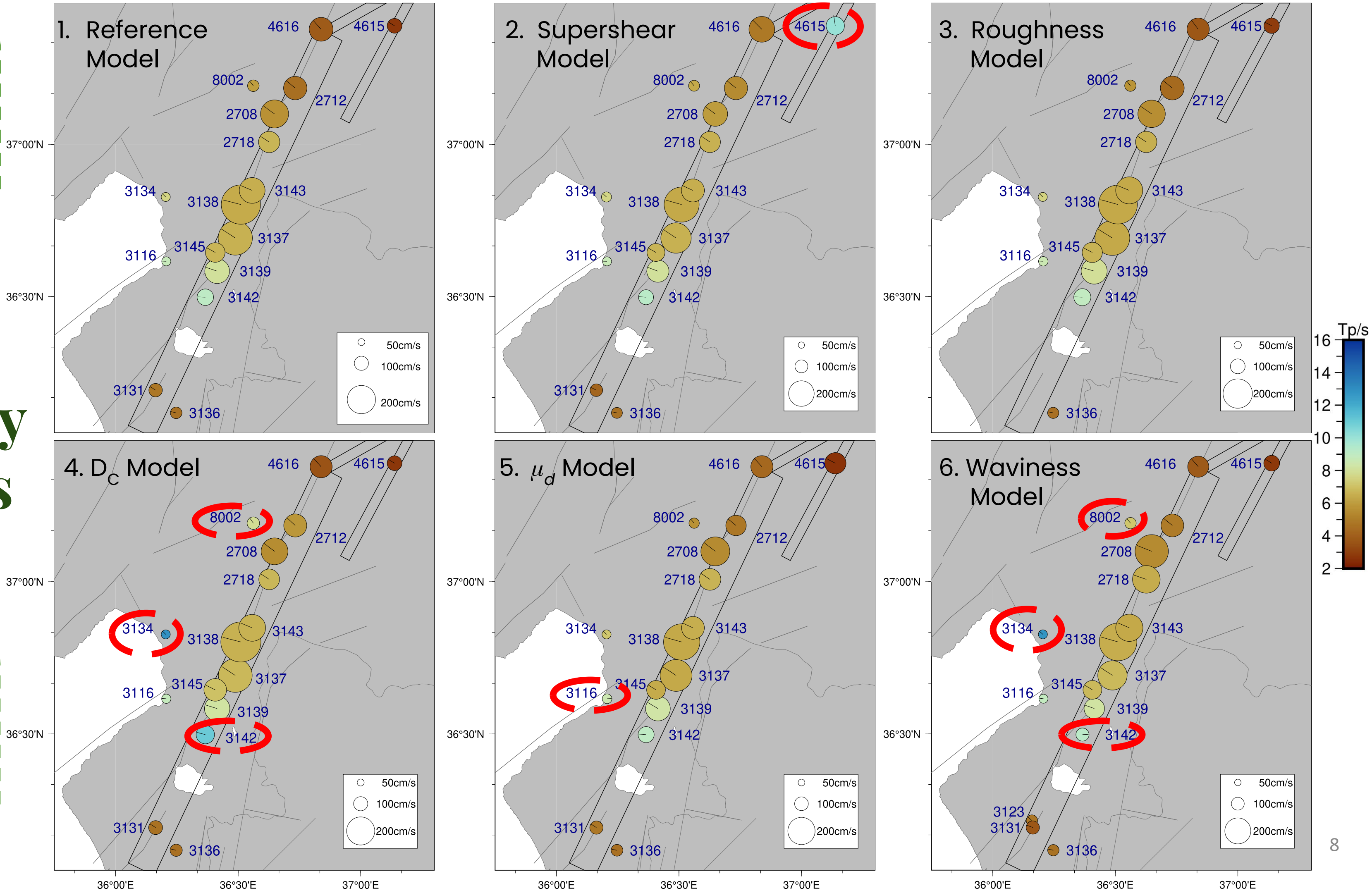

Pulse Property Comparison

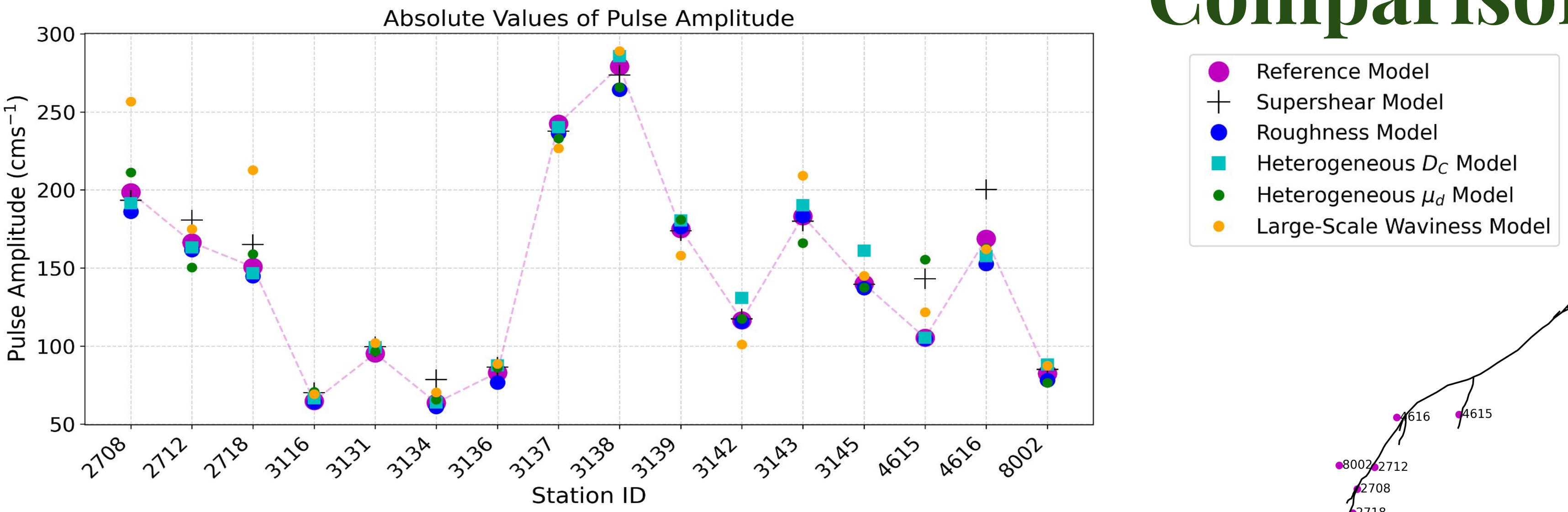

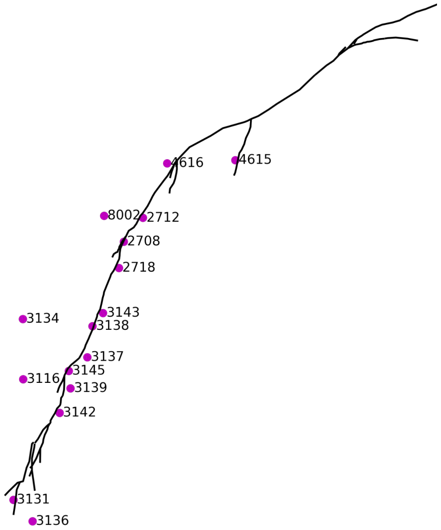

Pulse **amplitude variability** is **captured** well across all models

Pulse Property Comparison

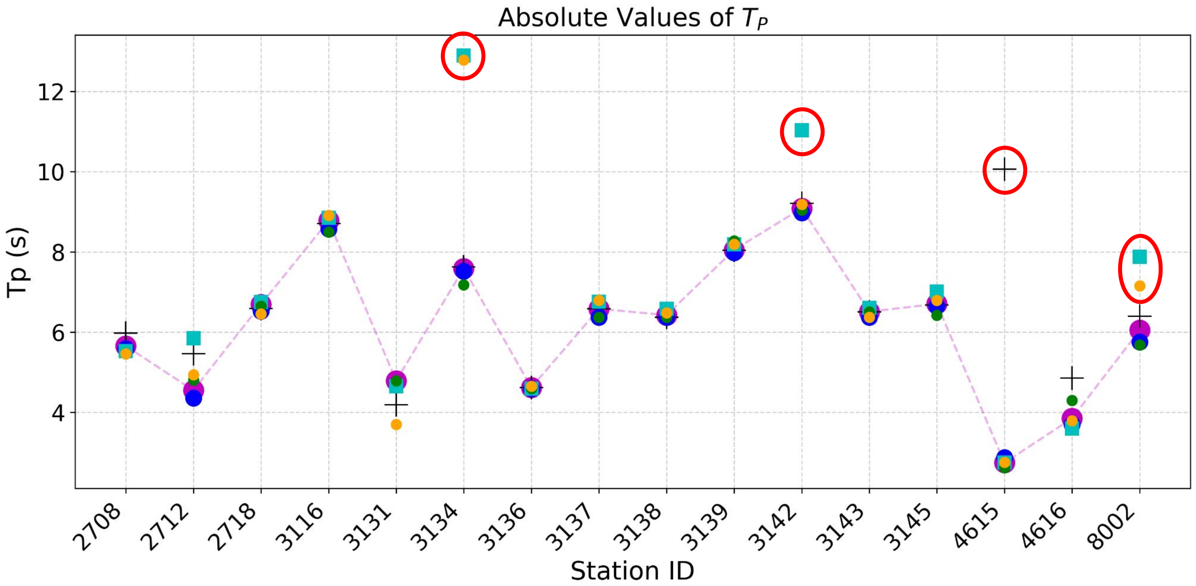

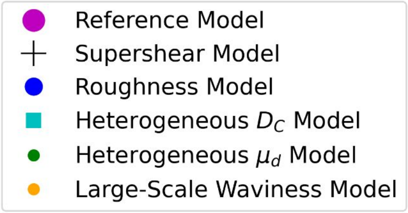

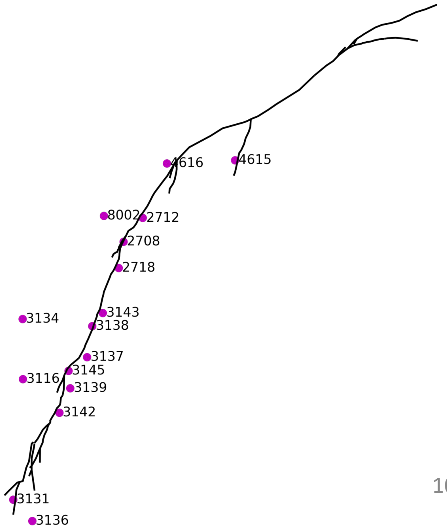

Pulse **period variability** is **increased** by **D_c heterogeneities** and **waviness** at a **few stations**

Pulse Property Comparison

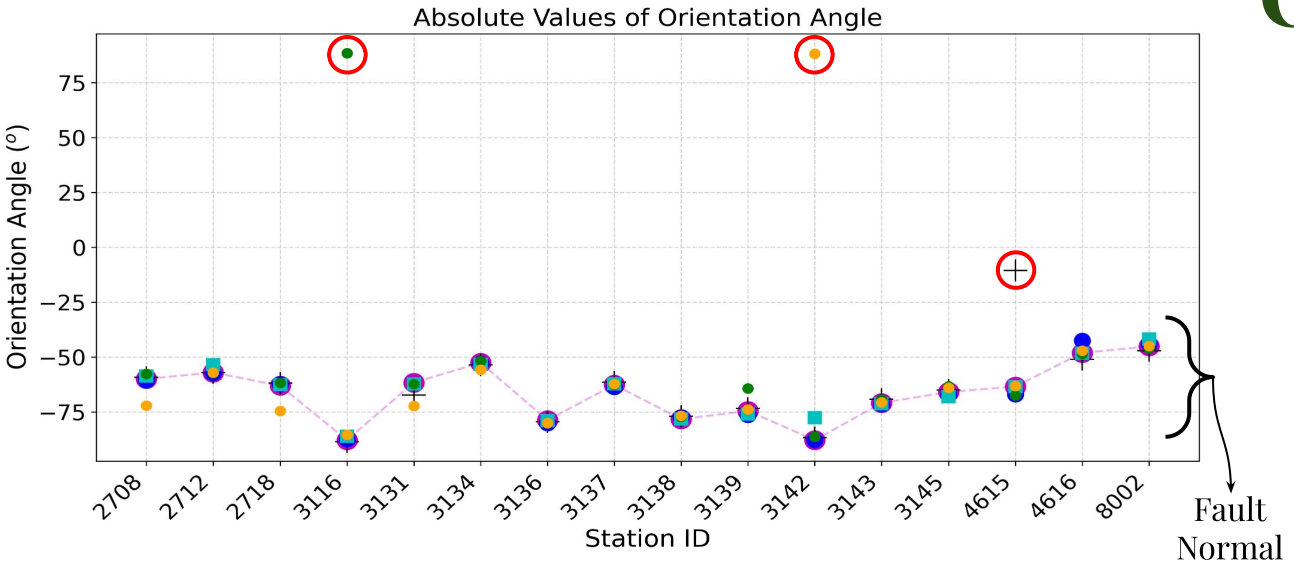

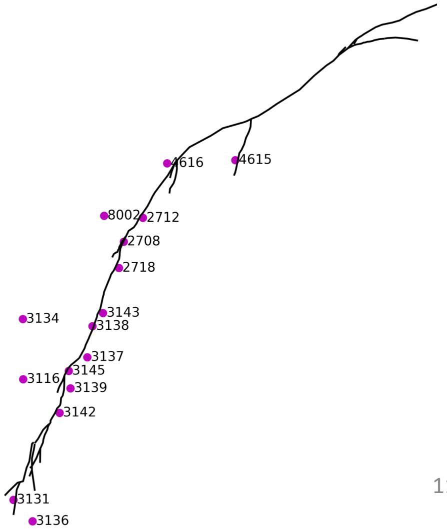

Pulse **orientation variability** is **captured** at 3 stations

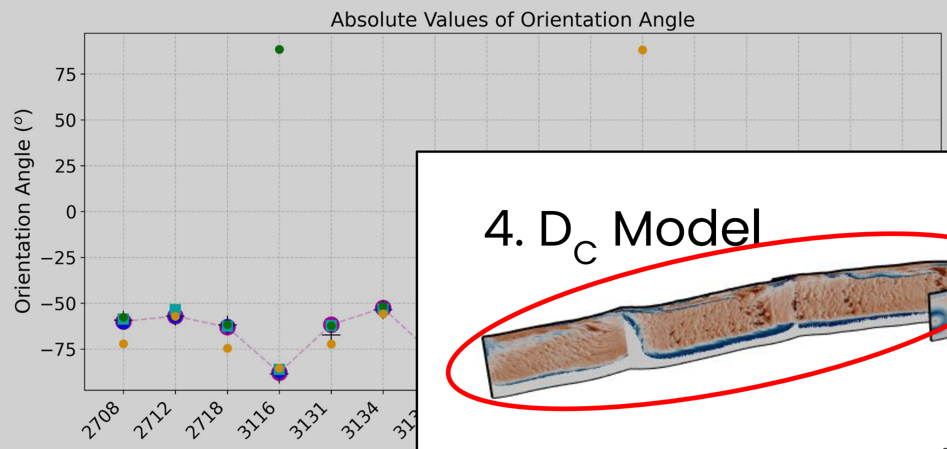

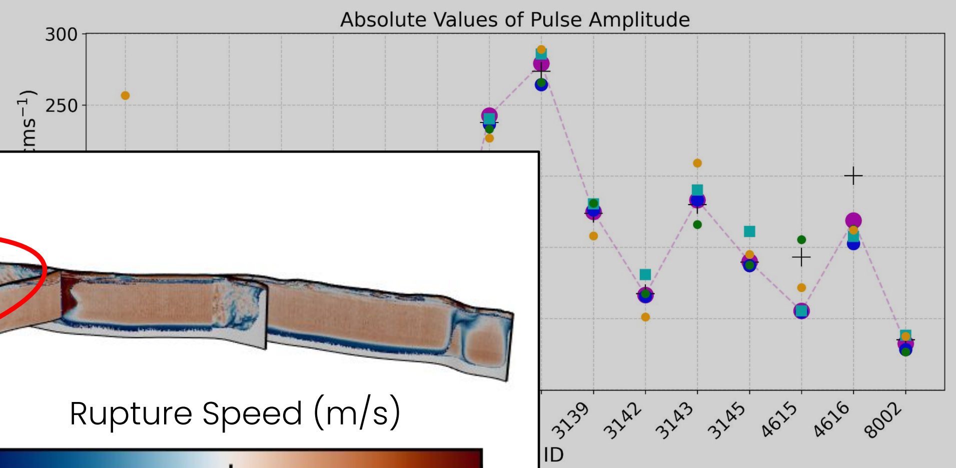

Pulse Prope
Comparis

Reference Model
Supershear Model
Roughness Model
Heterogeneous D_C Model
Heterogeneous μ_d Model
Large-Scale Waviness Model

4. D_C Model

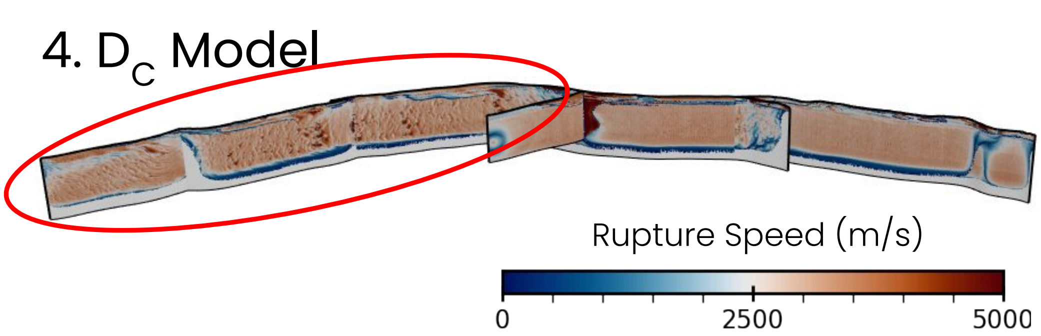

Heterogeneous μ_d and **D_c** both **change fracture energy**, but **only D_c** variability introduces **local, episodic supershear** rupture **affecting pulse properties**

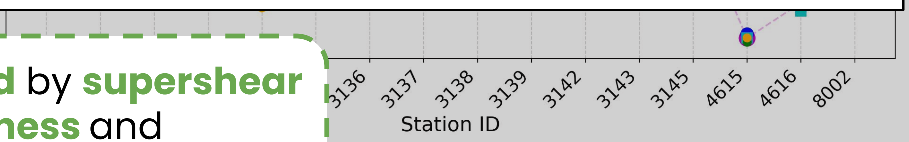

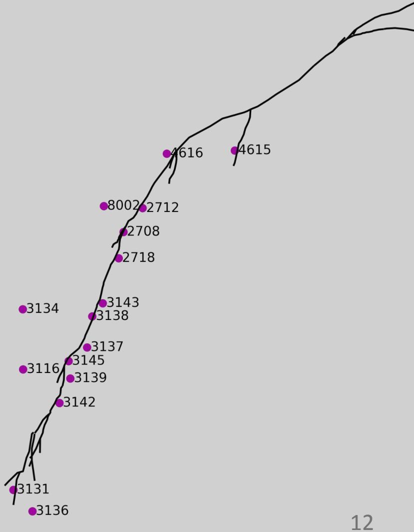

Pulse properties are **impacted** by **supershear rupture speeds**, **waviness** and **D_c heterogeneities**

Fracture Network

Triggered Fractures Case (Mw 6)

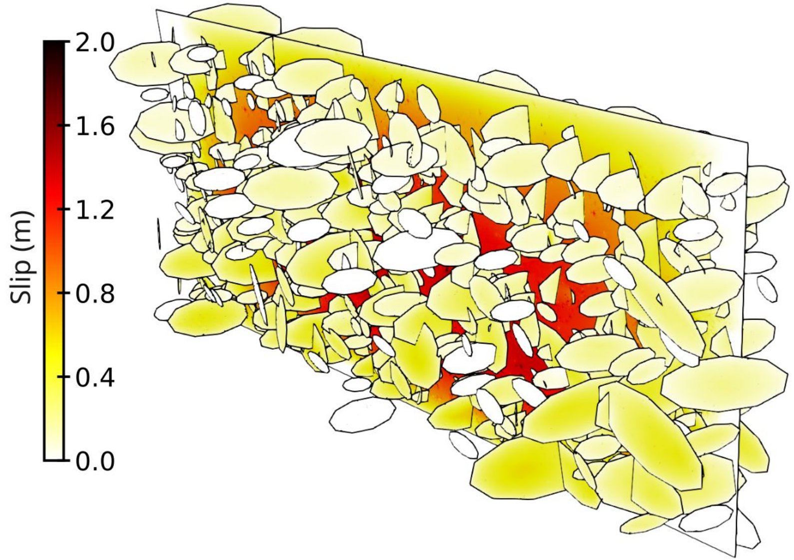

Fault-Only Case (Mw 5.94)

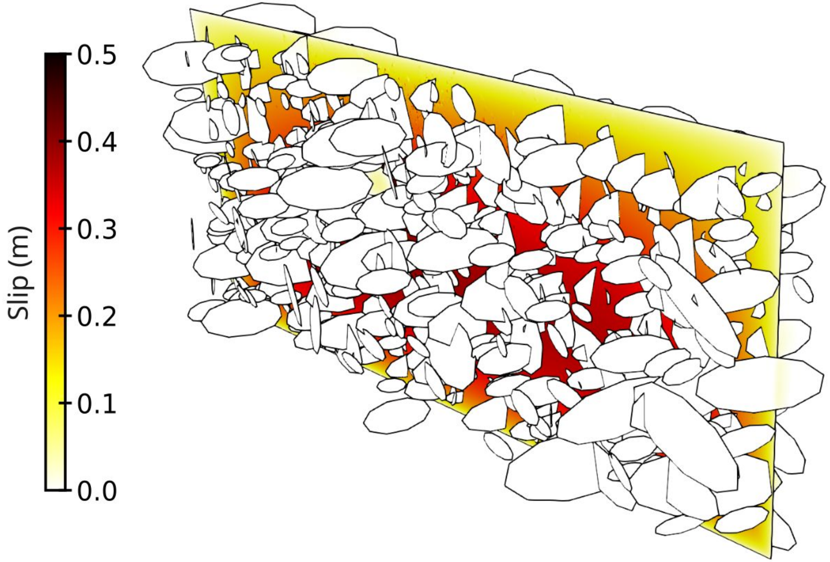

Based on Gabriel et al. (2024)

Fracture Network

Triggered Fractures Case (Mw 6)

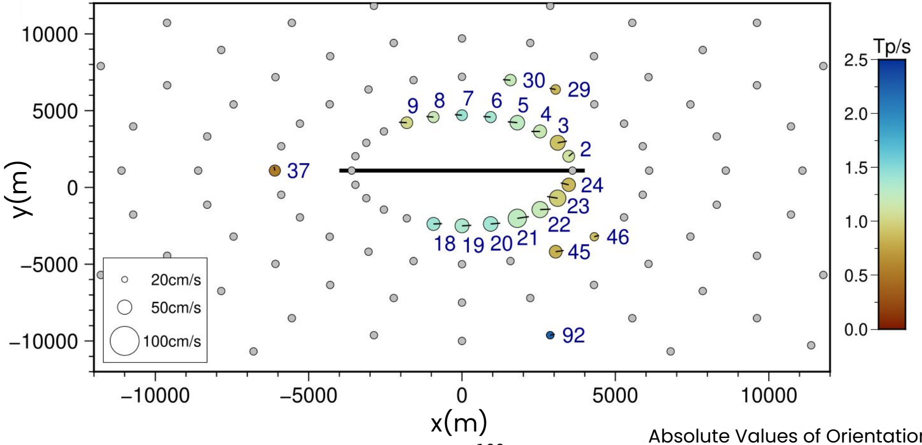

Fault-Only Case (Mw 5.94)

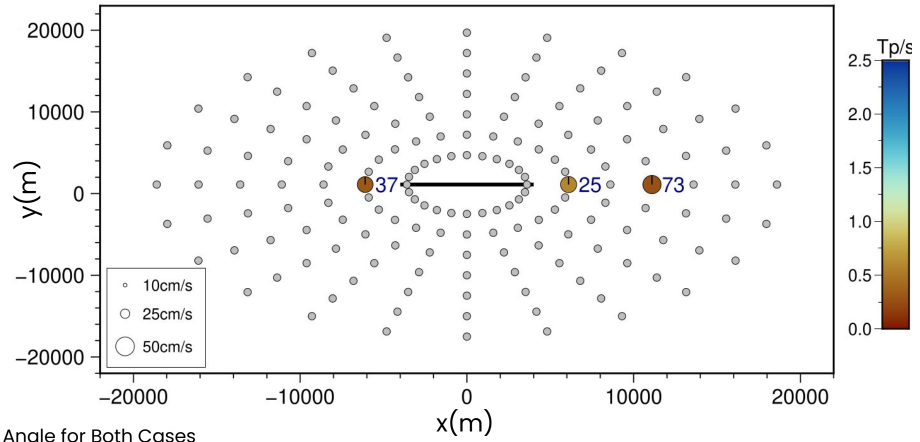

+ Triggered Fractures Case

+ Fault Only Case

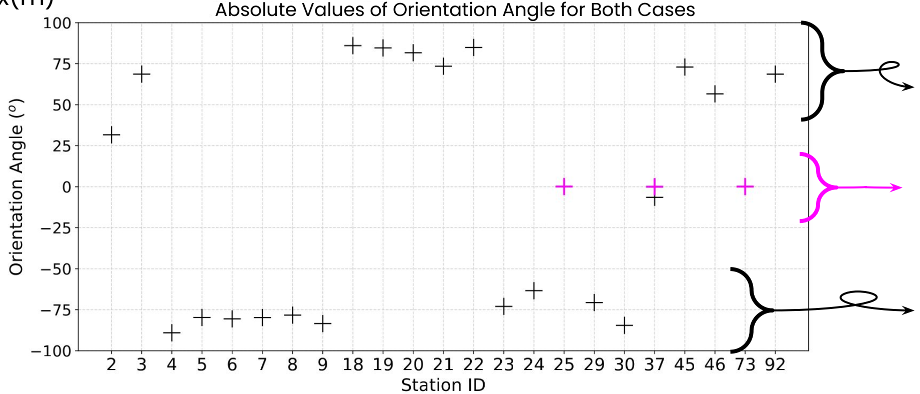

Fault Parallel

Fault Normal

Fault Parallel

Fracture network **improves** the pulse **variability**

Summary

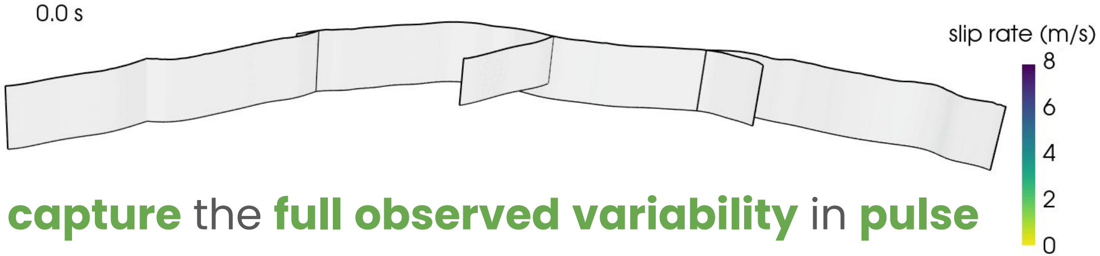

- **None** of our large-scale models **capture** the **full observed variability** in **pulse properties**

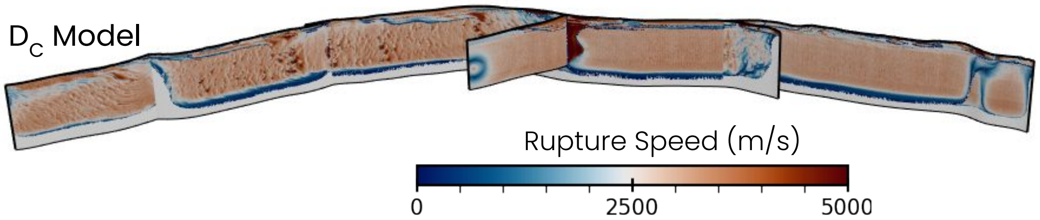

- Local **Supershear rupture speed** changes **pulse period** and **orientation** at station **4615**, but at no other station

- **D_c heterogeneity** and **large-scale fault waviness impact** overall pulse **period** and **orientation variability**

- **Fracture network impacts** variability in **pulse orientation**

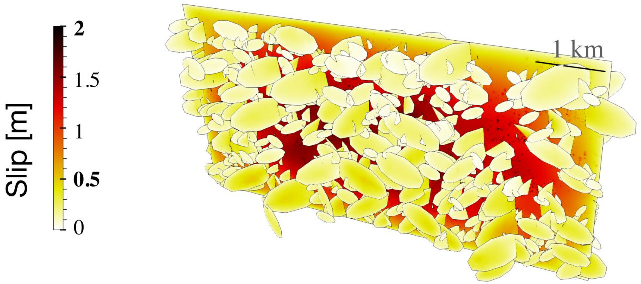

Preprint

https://eartharxiv.org/repository/view/11581/

R.Preca@lmu.de

Supplementary Slides

Moment Rate Release

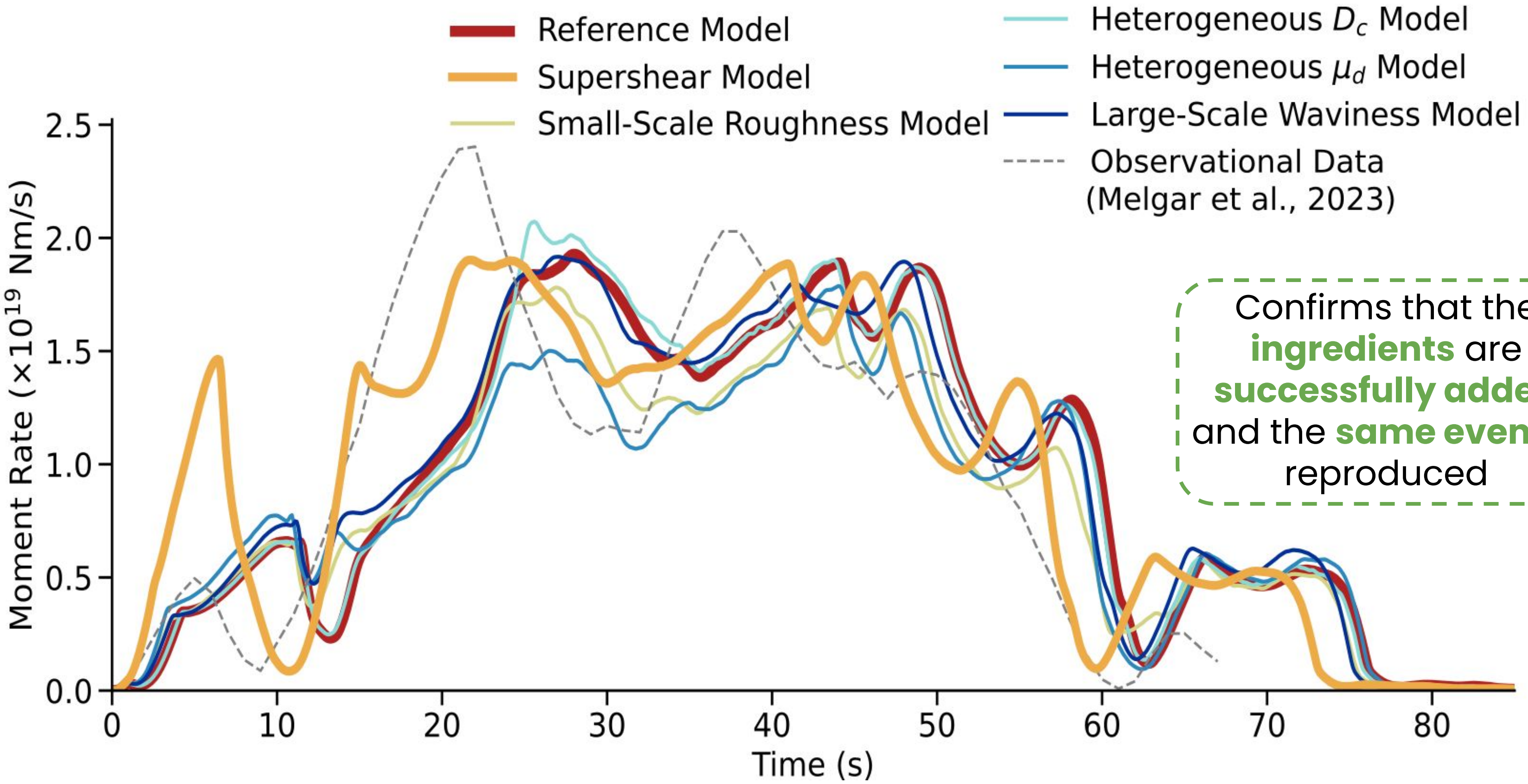

Confirms that the **ingredients** are **successfully added** and the **same event** is reproduced

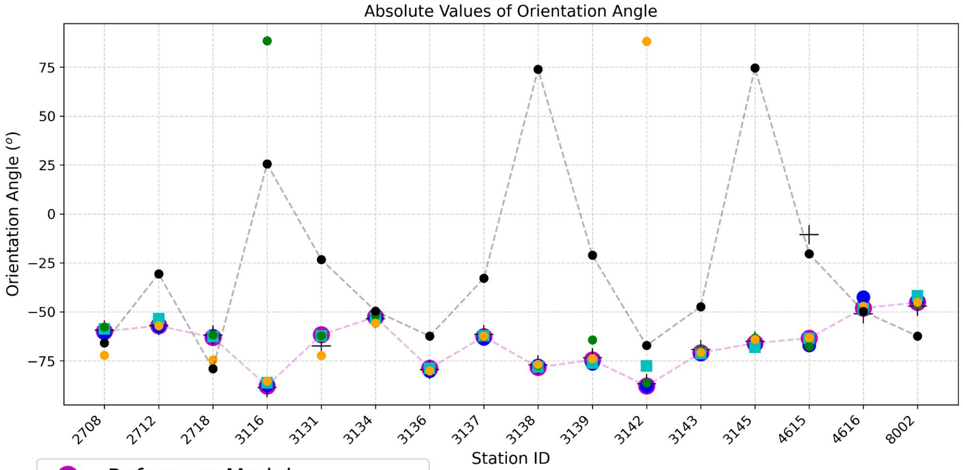

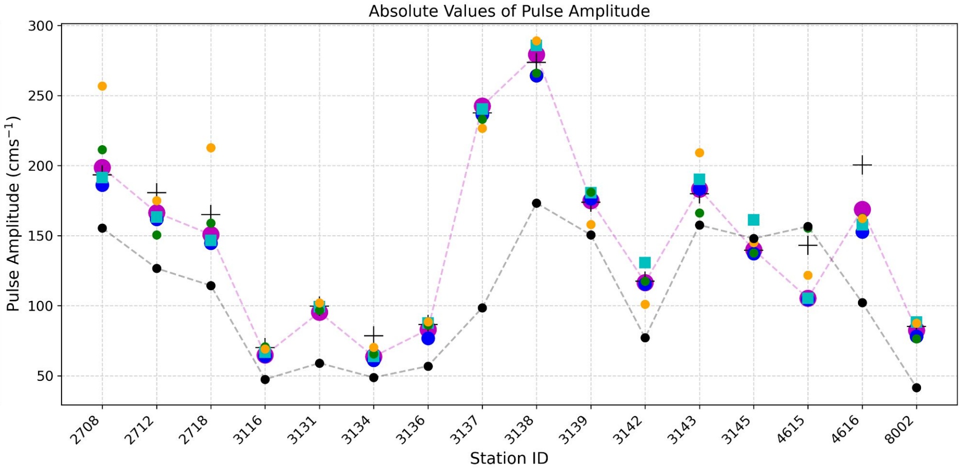

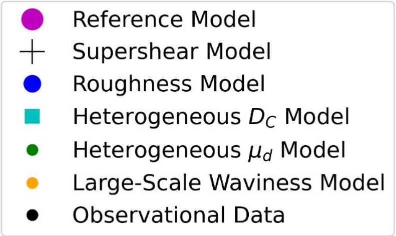

Pulse Property Comparison

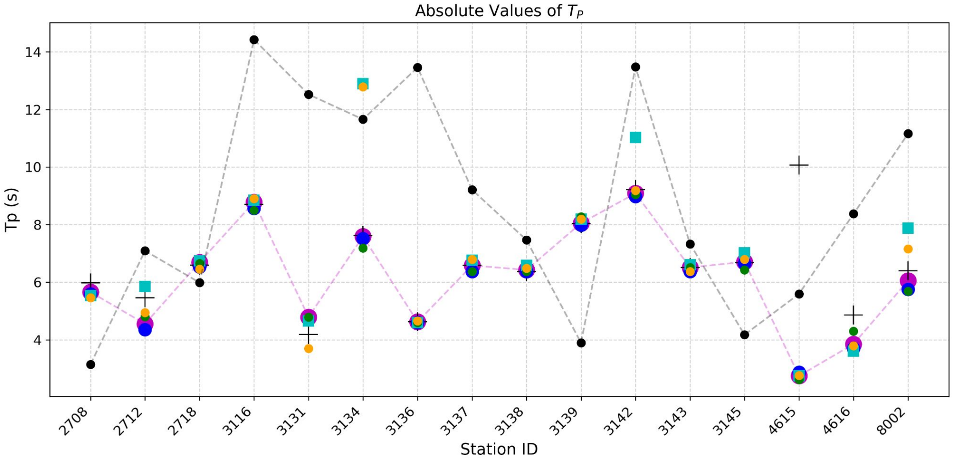

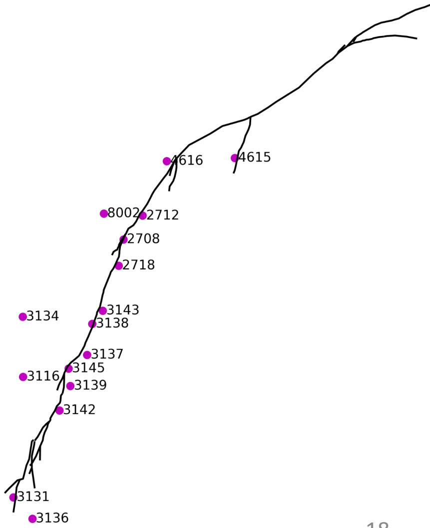

Fourier Spectra

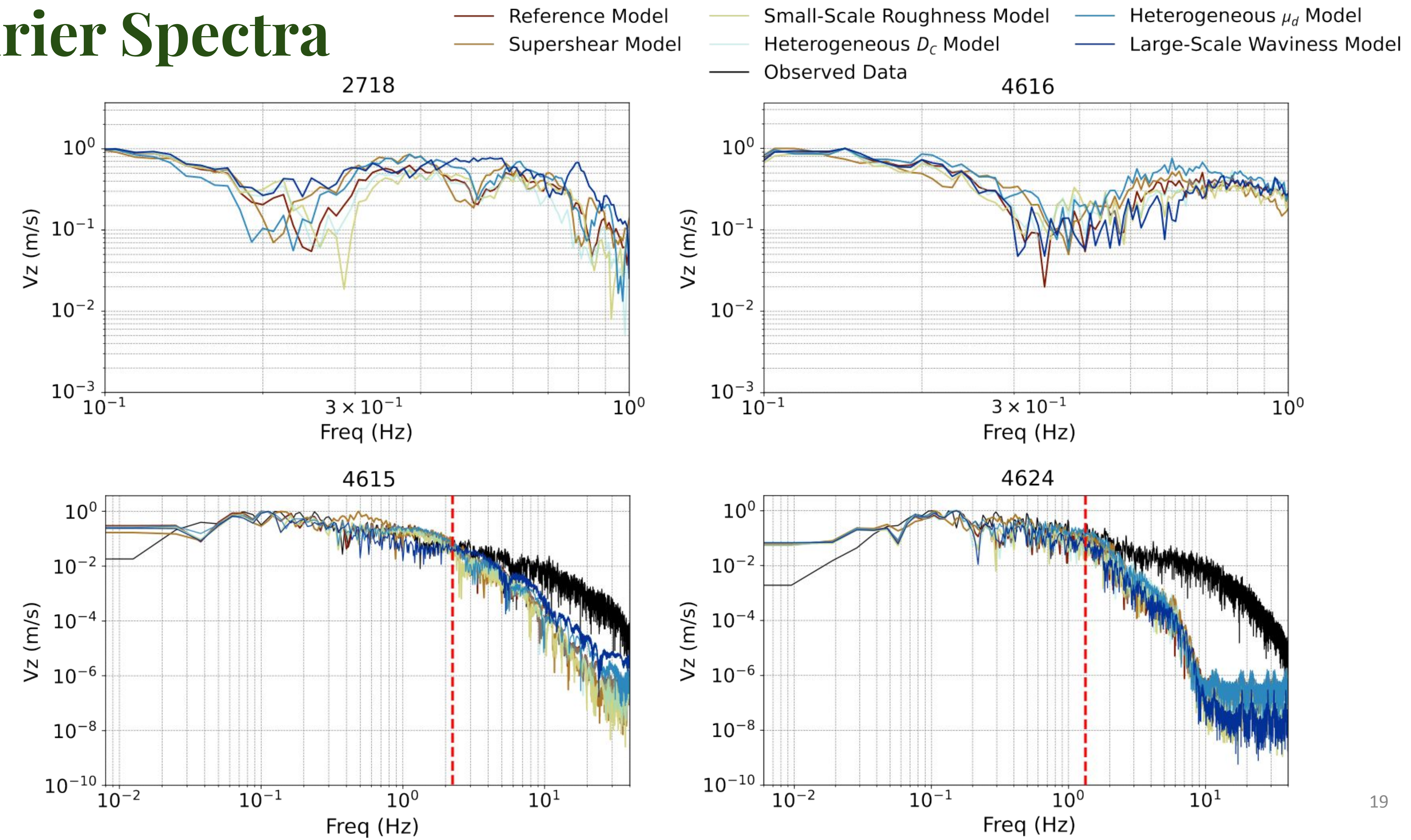

Relative Pre-Stress Ratio (R)

1. Reference Model

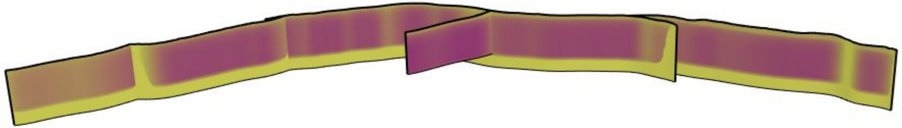

2. Supershear Model

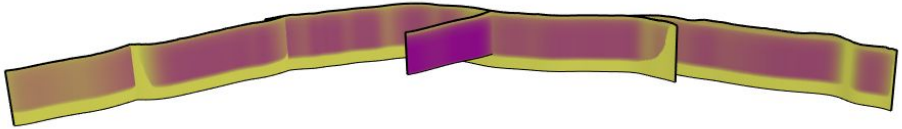

3. Roughness Model

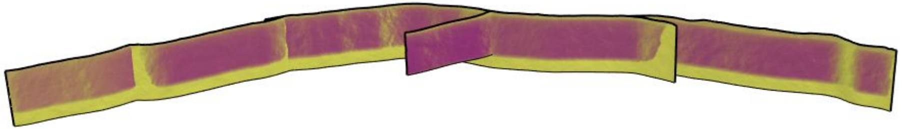

4. D_C Model

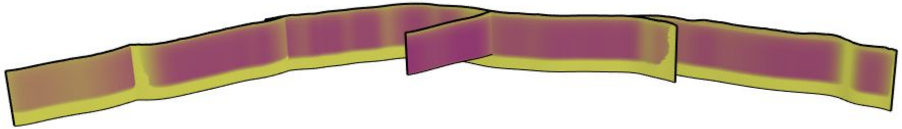

5. μ_d Model

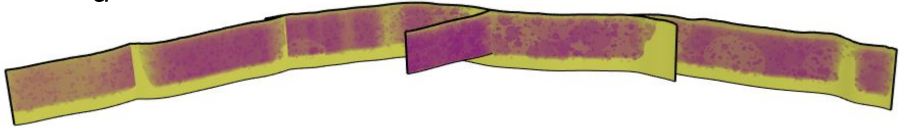

6. Waviness Model

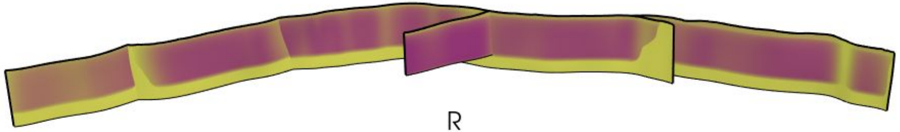

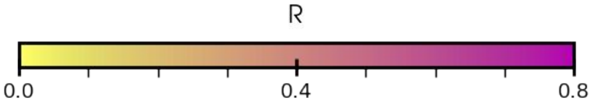

Difference in Prescribed Relative Pre-Stress Ratio (R_o) from Reference Model

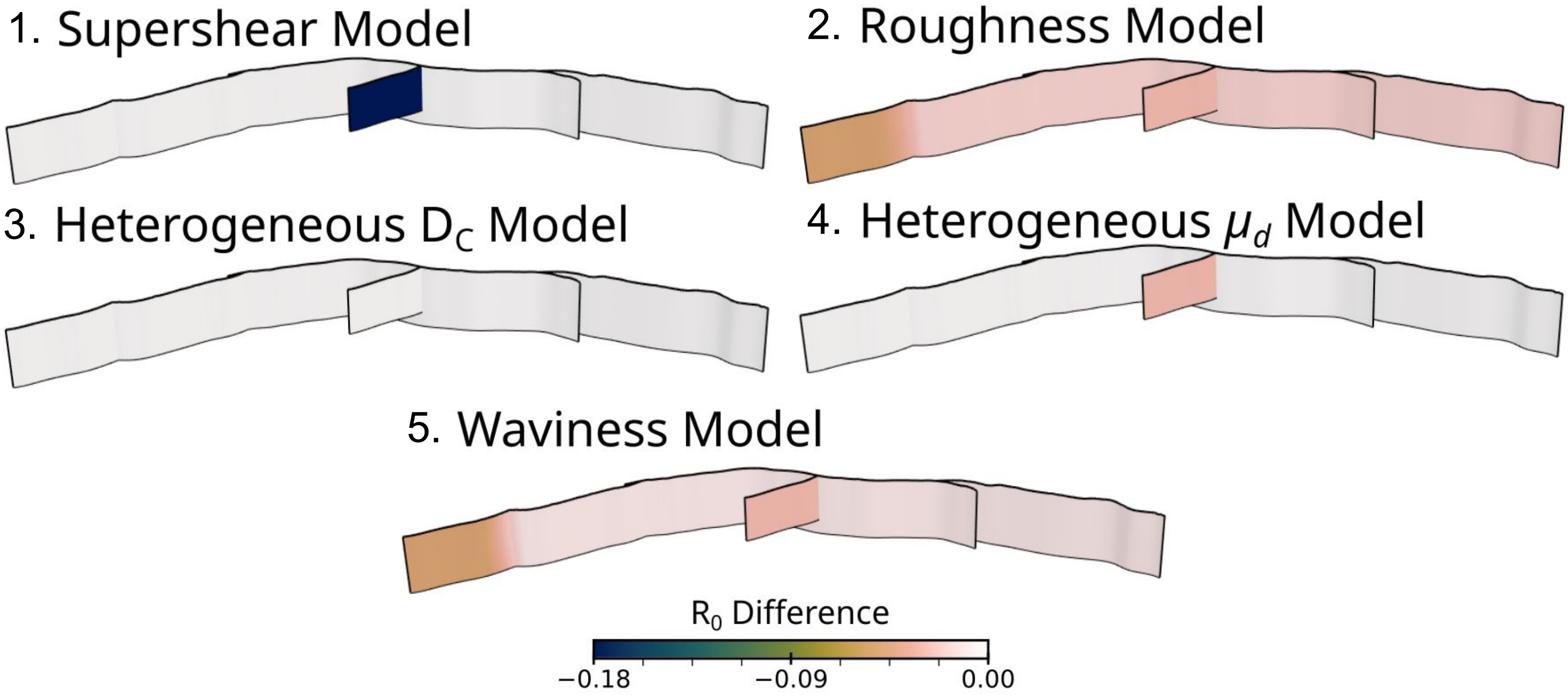

Fault Outputs - Final Slip

1. Reference Model

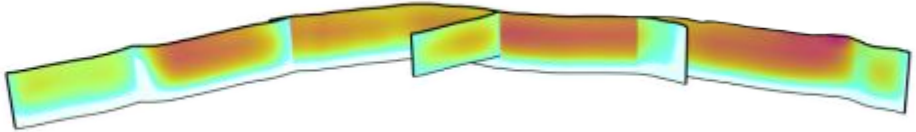

2. Supershear Model

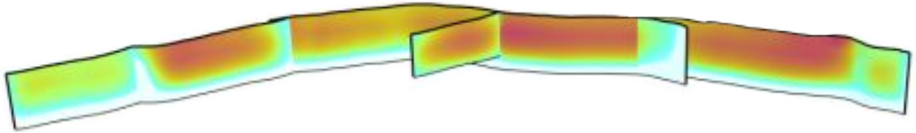

3. Roughness Model

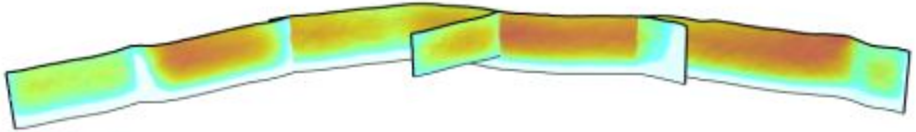

4. D_C Model

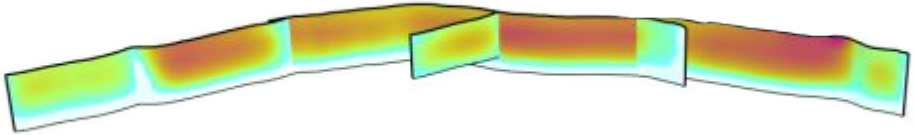

5. μ_d Model

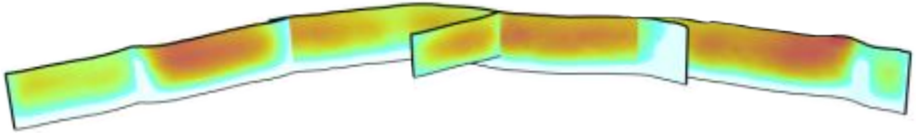

6. Waviness Model

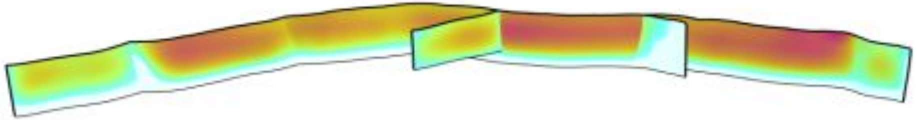

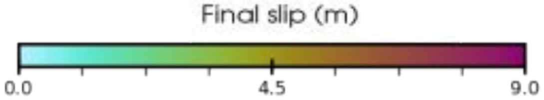

Fault Outputs - Difference in Final Slip from Reference Model

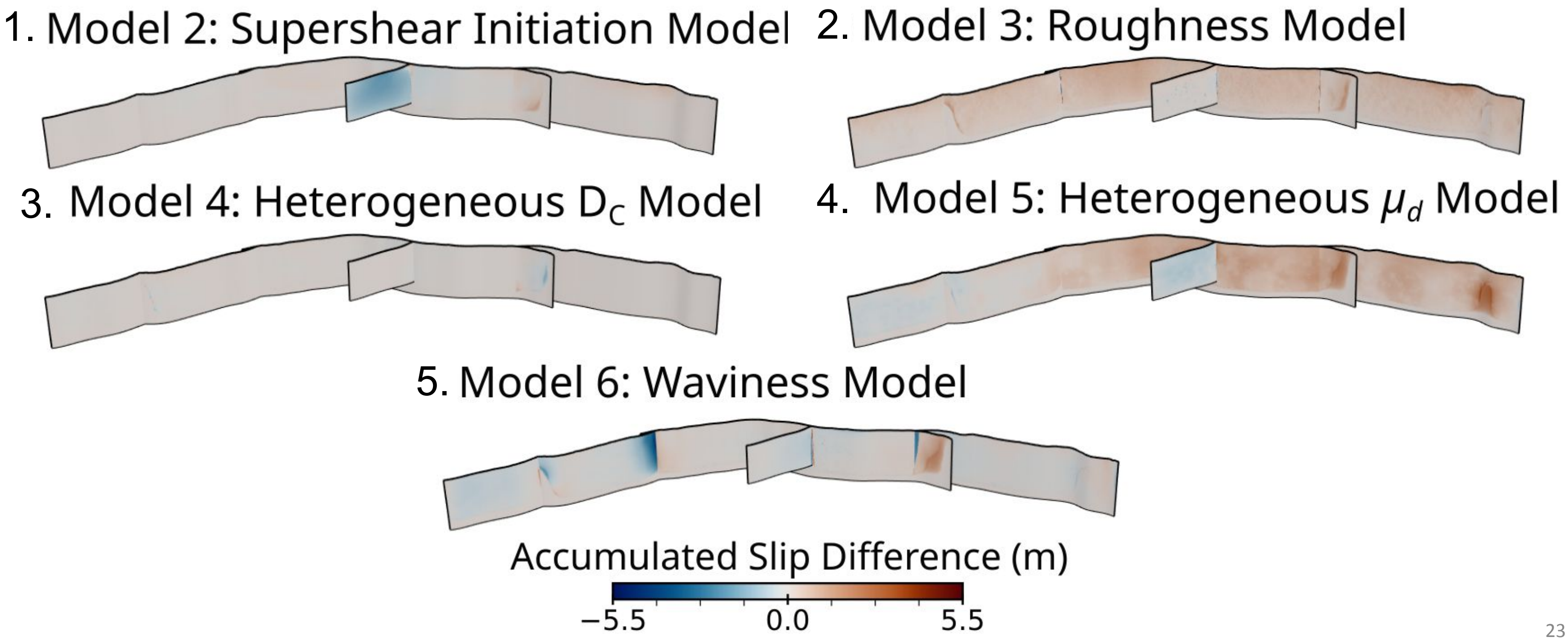

Fault Outputs - Peak Slip Rate

1. Reference Model

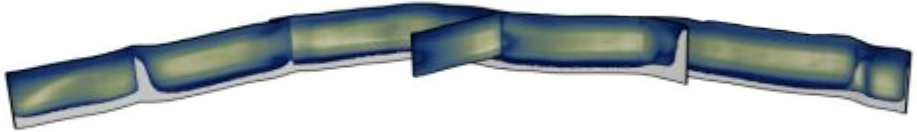

2. Supershear Model

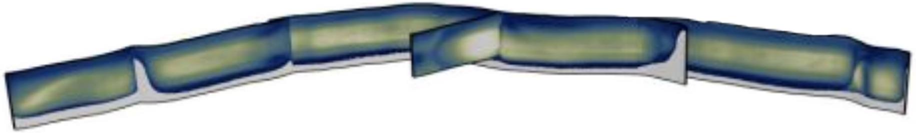

3. Roughness Model

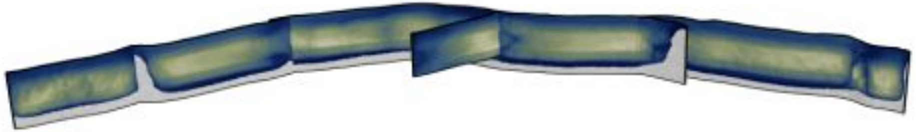

4. D_C Model

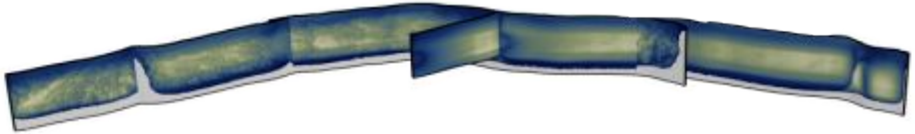

5. μ_d Model

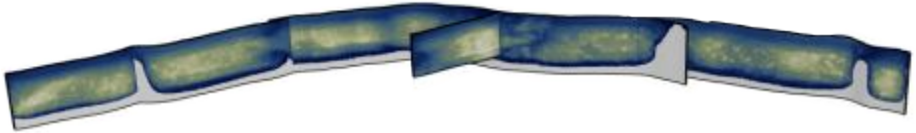

6. Waviness Model

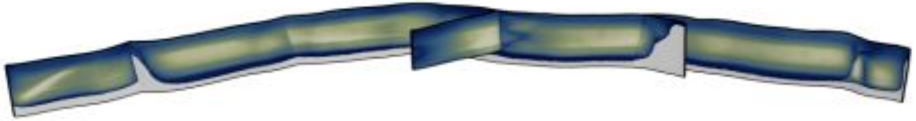

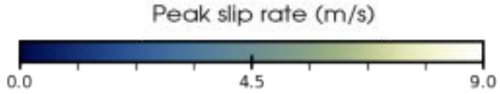

Fault Outputs - Difference in Peak Slip Rate from Reference Model

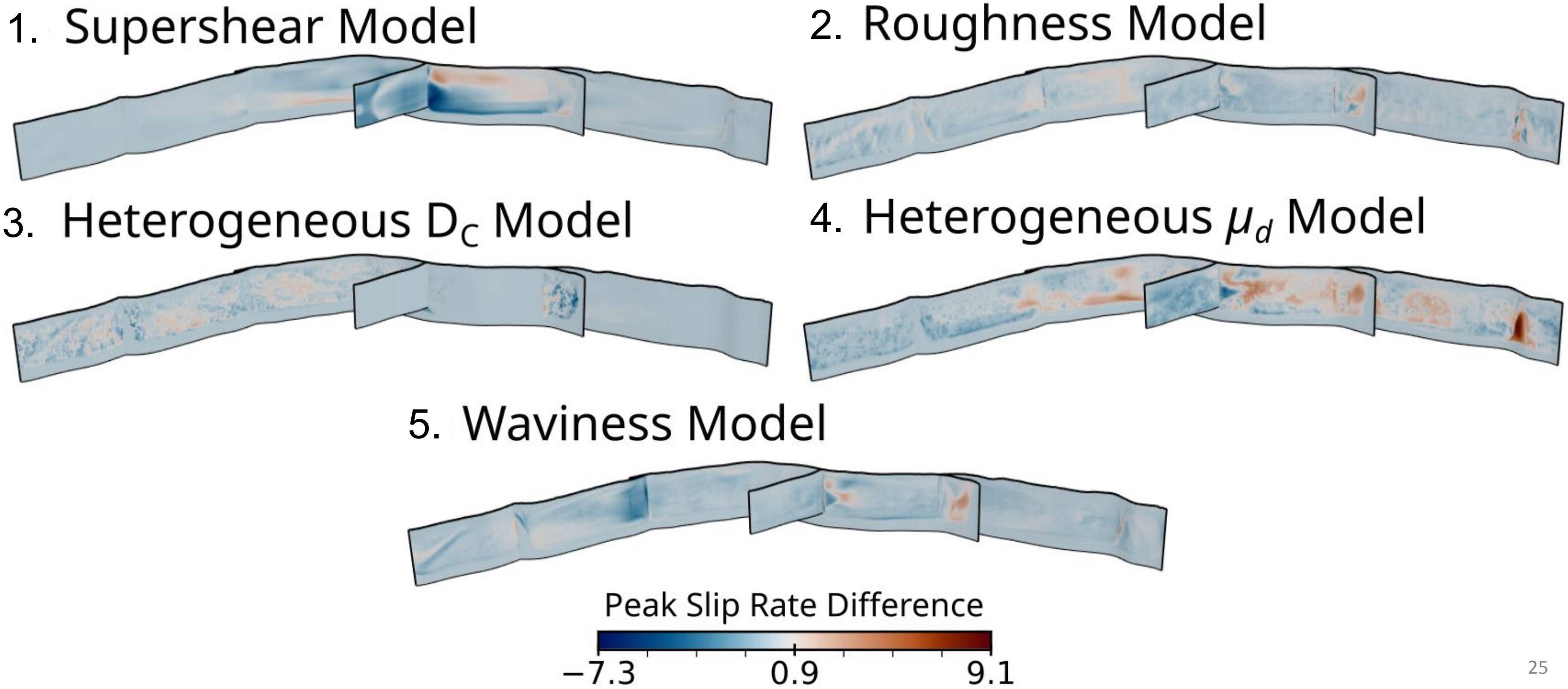

Shahi & Baker (2014) Pulse Extraction Method

- The 2 horiz. components are scaled
  - Defines the type of **wavelet** that will be used for the **Continuous Wavelet Transform (CWT)**

- In **freq - time domain** → see which frequencies dominant at which time step
  - Produce **coefficients** → how well **Daubechies wavelet** matches signal

- Conclude **best 5 coefficients** → find their **direction** & ∴ overall signal with pulse and pulse direction

- This gives the **best fitting wavelet** to the original signal

- **Pulse criterion** applied to find the best of the 5 options

Shahi & Baker (2014) Pulse Extraction Method

- Make use of: **energy ratio** of **residual** & **OG** GM
  : **PGV ratio** of **residual** & **OG** GM
  : **PGV** of **OG** GM

~> these show **strength** of **extracted pulse**

  - **Low energy ratio** ⇒ **pulse** removed from **OG** GM **contributes significantly to energy** of **GM**
  - **Lower PGV ratio** ⇒ **pulse responsible** for **peak velocity** of GM
  - **Need PGV of recorded motion** to help **distinguish** between **weak** motions and **pulse-like motions**

- **Principal component** analysis → captures most of the info expressed by variables individually

$$PC = 0.63 \times (\text{PGV ratio}) + 0.77 \times (\text{energy ratio})$$

- **Pulse indicator**:

$$PI = 9.384(0.76 - PC - 0.0616PGV)(PC + 6.914e\text{-}4PGV - 1.072) - 6.179 \qquad > 0 \Rightarrow \text{Pulse-like}$$

- Pulses by **directivity** effects **arrive earlier** ∴ Include **criterion** to **exclude late arriving pulses** to only extract directivity pulses